

# Study of transversity GPDs from pseudoscalar mesons production at EIC of China

S.V.Goloskokov<sup>\*1</sup>, Ya-Ping Xie<sup>†2,3</sup>, and Xurong Chen<sup>‡2,3,4</sup>

<sup>1</sup>Bogoliubov Laboratory of Theoretical Physics, Joint Institute for Nuclear Research, Dubna 141980, Moscow region, Russia

<sup>2</sup>Institute of Modern Physics, Chinese Academy of Sciences, Lanzhou 730000, China

<sup>3</sup>University of Chinese Academy of Sciences, Beijing 100049, China

<sup>4</sup>Institute of Quantum Matter, South China Normal University, Guangzhou 510006, China

## Abstract

The exclusive  $\eta$  and  $\pi^0$  electroproduction is studied in the handbag approach based on Generalized Parton Distributions (GPDs) factorization. Predictions of  $\pi^0$  and  $\eta$  mesons are calculated for future Electron-Ion Collider of China (EicC) energy range using obtained cross sections we extract information on the transversity GPDs contributions to these processes.

## 1 Leptoproduction of pseudoscalar mesons

In this paper, we analyze pseudoscalar meson electroproduction ( $\pi^0$ ,  $\eta$ ) on the basis of handbag approach. Its essential ingredients are the Generalized Parton Distributions (GPDs) that were proposed in Refs [1, 2, 3] and provide an extensive information on the hadron structure. GPDs are complicated nonperturbative objects which depend on  $x_B$  -the momentum fraction of proton carried by parton,  $\xi$ - skewness and  $t$ - momentum transfer. GPDs are connected in the forward limit with Parton Distribution Functions (PDFs), they contain information about hadron form factors and the parton angular momentum [4]. They give information

---

<sup>\*</sup>goloskv@theor.jinr.ru

<sup>†</sup>xieyaping@impcas.ac.cn

<sup>‡</sup>xchen@impcas.ac.cn

on 3D structure of the hadrons, see e.g. [5]. More details on GPDs can be found e.g. in [6, 7, 8, 9].

GPDs were proposed to investigate exclusive reactions such as deeply virtual Compton scattering (DVCS) [4, 10, 11], time-like Compton scattering (TCS) [12, 13, 14] and deeply virtual meson production (DVMP) [6, 7]. Such processes at large photon virtuality  $Q^2$  can be factorized into the hard subprocess that can be calculated perturbatively and the GPDs [4, 10, 11]. Generally, this factorization was proved in the leading-twist amplitude with longitudinally polarized photon. This factorization formulae is valid up to power corrections of the order  $1/Q$  to the leading twist results which are unknown.

Study of exclusive meson electroproduction is one of the effective way to access GPDs. Experimental study of  $\pi^0$  production was performed by CLAS [15] and COMPASS [16]. For  $\eta$  production CLAS results are available at [17]. These experimental data can be adopted to constrain the models of GPDs. On the other hand, Electron-Ion Colliders (EICs) are the next generation collider to study of nucleon structure. USA and China both design to build the EICs in future [18, 19, 20]. The GPDs property is one of the most important aims to investigate for the EICs [21].

Theoretical investigation of DVMP in terms of GPDs is based on the handbag approach where, as mentioned before, the amplitude is factorized into the hard subprocess and GPDs [2, 3, 4, 10] see Fig. 1. This amplitude has an ingredient the non-perturbative meson Distribution Amplitudes, which probe the two-quark component of the meson wave functions. One of the popular way to construct GPDs is adopting so called Double Distribution (DD) [22] which construct  $\xi$  dependencies of GPDs and connect them with PDFs, modified by  $t$ - dependent term. The handbag approach with DD form of GPDs was successfully applied to the light vector mesons (VM) leptonproduction at high photon virtualities  $Q^2$  [23] and the pseudoscalar mesons (PM) leptonproduction [24].

In this work, we continue our previous study of  $\pi^0$  production [25] at the kinematics for EIC in China (EicC) based on the handbag approach. As it was shown in [24] the leading twist longitudinal cross section  $\sigma_L$  is rather small with respect to the predominant contribution determined by transversely polarized photons  $\sigma_T$ . This result was proved experimentally by JLab Hall A collaboration [26]. The transversity dominance  $\sigma_T \gg \sigma_L$  is confirmed in [25] at all EicC energy ranges for  $\pi^0$  production.

This paper is organized as follows. In section 2, we discuss the contributions to the meson production amplitudes from the transversity GPDs  $H_T, \bar{E}_T$  [27]. Within the handbag approach, the transversity GPDs together with the twist-3 meson wave functions [27] contribute to the amplitudes with transversely polarized photons which produce transverse cross sections  $\sigma_T$ . They give essential contribution to the cross sections that are consistent with experiment [15, 16].

In section 3, we consider two models for transversity GPDs that give results for the cross sections of the  $\pi^0$  and  $\eta$  leptonproduction that are consistent with

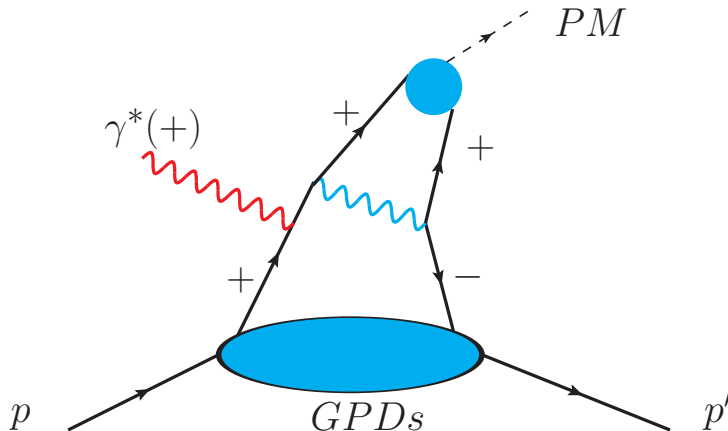


Figure 1: The handbag diagram for the meson electroproduction off proton. Parton helicities for transversity GPDs contribution are shown.

experiment at CLAS and COMPASS energies [15, 16, 17]. Predictions for  $\eta$  cross section at EicC energies are done. Later on we extract information on the transversity GPDs contribution for these reactions. We discuss possibility to perform  $u, d$  flavor separation for transversity GPDs  $H_T$  and  $\bar{E}_T$  using  $\pi^0$  and  $\eta$  cross sections [28, 29]. Finally, We give some discussion and conclusions in section 4.

## 2 Handbag approach. Properties of meson production amplitudes

The process amplitude in the handbag approach is depicted in Fig. 1. In handbag approach, the meson photoproduction amplitude is factorized into a hard subprocess amplitude  $\mathcal{H}$  which is shown in the upper part of Fig. 1 and GPDs  $F$  which includes information on the hadron structure at sufficiently high  $Q^2$ . For the leading twist amplitude, with longitudinally polarized photons, its factorization has been proved [2, 3].

In what follows, we consider the twist-3 contributions from transversity GPDs  $H_T$  and  $\bar{E}_T$  as well. Factorization for these twist-3 amplitudes is an assumption now. However factorization models give results which are consistent with experiment [27].

In handbag method, the subprocess amplitude is calculated employing the modified perturbative approach (MPA) [30]. The power  $k_\perp^2/Q^2$  correction is considered in the propagators of the hard subprocess  $\mathcal{H}$  together with the nonperturbative  $\mathbf{k}_\perp$ -dependent meson wave functions [31]. The gluonic corrections are regarded as the form of the Sudakov factors. Resummation of the Sudakov factor can be done in the impact parameter space [30].

The unpolarized  $ep \rightarrow e(\pi^0, \eta)p$  cross section can be decomposed into a number of partial cross sections which are expressed in terms of the  $\gamma^*p \rightarrow (\pi^0, \eta)p$  helicity amplitudes. They have the following forms

$$\begin{aligned}
\frac{d\sigma_L}{dt} &= \frac{1}{\kappa}(|M_{0+,0+}|^2 + |M_{0-,0+}|^2), \\
\frac{d\sigma_T}{dt} &= \frac{1}{2\kappa}(|M_{0-,++}|^2 + 2|M_{0+,++}|^2), \\
\frac{d\sigma_{LT}}{dt} &= -\frac{1}{\sqrt{2}\kappa}\text{Re}[M_{0-,++}^* M_{0-,0+}], \\
\frac{d\sigma_{TT}}{dt} &= -\frac{1}{\kappa}|M_{0+,++}|^2.
\end{aligned} \tag{1}$$

Here  $\kappa$  is the phase space factor, it reads

$$\kappa = 16\pi(W^2 - m^2)\sqrt{\Lambda(W^2, -Q^2, m^2)}. \tag{2}$$

$\Lambda(x, y, z)$  is expressed as  $\Lambda(x, y, z) = (x^2 + y^2 + z^2) - 2xy - 2xz - 2yz$ .  $\sigma_{LT}$  is the interference contributions of the longitudinal and transverse amplitudes and  $\sigma_{TT}$  contains transverse amplitudes only.

The leading twist amplitudes  $M_{0-,0+}$  and  $M_{0+,0+}$  are listed in our previous paper [25]. The transversity amplitudes that are essential in our study can be written in terms of convolutions as

$$\begin{aligned}
M_{0-,++} &= \frac{e_0}{Q}\sqrt{1 - \xi^2}\langle H_T \rangle, \\
M_{0+,++} &= -\frac{e_0}{Q}\frac{\sqrt{-t'}}{4m}\langle \bar{E}_T \rangle,
\end{aligned} \tag{3}$$

where  $e_0 = \sqrt{4\pi\alpha}$  with  $\alpha$  is the electronic-magnetic coupling. The other variables are defined as

$$\xi = \frac{x_B}{2 - x_B}\left(1 + \frac{m_P^2}{Q^2}\right), \quad t' = t - t_0, \quad t_0 = -\frac{4m^2\xi^2}{1 - \xi^2}. \tag{4}$$

$x_B$  is the Bjorken variable which is given as  $x_B = Q^2/(W^2 + Q^2 - m^2)$ .  $m$  is the proton mass and  $m_P$  is the pseudoscalar meson mass.

The GPDs  $F(x, \xi, t)$  are calculated as the integration of the double distributions function [22]

$$F(x, \xi, t) = \int_{-1}^1 d\rho \int_{-1+|\rho|}^{1-|\rho|} d\gamma \delta(\rho + \xi\gamma - x) f(\rho, t) v(\rho, \gamma, t). \tag{5}$$

For the valence quark double distributions read as

$$v(\rho, \gamma, t) = \frac{3}{4} \frac{[(1 - |\rho|)^2 - \gamma^2]}{(1 - |\rho|)^3}. \tag{6}$$

The  $t$ -dependence in PDFs  $f$  is expressed as the Regge form

$$f(\rho, t) = N e^{(b-\alpha' \ln \rho)t} \rho^{-\alpha(0)} (1 - \rho)^\beta, \quad (7)$$

and  $\alpha(t) = \alpha(0) + \alpha' t$  is the corresponding Regge trajectory factor. The parameters in Eq. (7) are fitted from the known information about CTEQ6 PDF [32] e.g, or from the nucleon form factor analysis [33]. We consider  $Q^2$  evolution of GPDs via evolution of PDF in Eq. 7, see [23]. This form of evolution is proper near the forward limit. Generally in this work, the explicit form of GPDs evolution is not so important because we work at very limited  $Q^2$  interval.

It was found that for PM leptonproduction the contributions of the transversity GPDs  $H_T$  and  $\bar{E}_T = 2\tilde{H}_T + E_T$  are essential [27]. It determines the amplitudes  $M_{0-,++}$  and  $M_{0+,++}$  respectively, see Eq. (3). With the handbag approach the transversity GPDs are accompanied by a twist-3 PM wave functions in the hard amplitude  $\mathcal{H}$  [27] which is the same for both the  $M_{0\pm,++}$  amplitudes in Eq. (3). This property is demonstrated in Fig. 1, where the parton helicities of the subprocess amplitude  $\mathcal{H}$  are presented. For corresponding transversity convolutions we have forms:

$$\langle H_T \rangle = \int_{-1}^1 dx \mathcal{H}_{0-,++}(x, \dots) H_T; \quad \langle \bar{E}_T \rangle = \int_{-1}^1 dx \mathcal{H}_{0-,++}(x, \dots) \bar{E}_T. \quad (8)$$

There is a parameter  $\mu_P$  in twist-3 meson wave function that is large and enhanced by the chiral condensate. In our calculation, we use  $\mu_P = 2$  GeV at scale of 2 GeV.

More details of leading twist polarized GPDs  $\tilde{H}$  and  $\tilde{E}$  which contribute to the leading twist amplitudes with longitudinally polarized virtual photons can be found in paper [24, 27]. These amplitudes contribute to longitudinal cross section  $\sigma_L$  which is rather small with respect to transversity contribution  $\sigma_T$  for  $\pi^0$  and  $\eta$  production.

For additional information about transversity GPDs parameterization see [27] and [25]. The  $\pi^0$  estimations at EicC are presented in our previous paper [25]. Study of  $\eta$  meson leptonproduction can be performed within the handbag approach too, for details see [27].

### 3 Model results for $\pi^0$ and $\eta$ leptonproduction and convolution extraction from the data

We consider the transversity effects described in Eq. (8) and take into account the leading twist contribution in Eq. (1). The amplitudes are transferred from program produced by PARTONS collaboration codes [34] which was changed into Fortran employing results of GK model for GPDs [27].

In our previous paper [25], two models for transversity GPDs were analyzed. Model-1 was applied in [27] and described fine low energy CLAS data [15], but gave results about two times larger with respect to COMPASS data [16]. It was

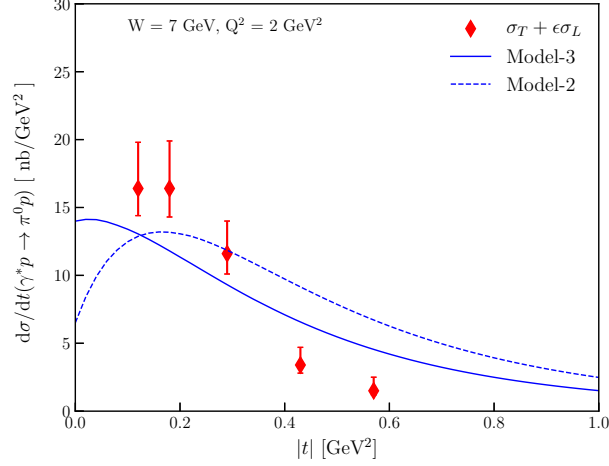


Figure 2: Models results at COMPASS kinematics. Experimental data are taken from [16], dashed line represents the results of Model-2 and solid curve indicates the prediction of Model-3

the reason to change GPDs parameters, especially for  $\bar{E}_T$  contribution that is important in  $\sigma_T$  and  $\sigma_{TT}$  cross sections. Some changes were done for  $H_T$  as well. The parameters for new model labeled as Model-2 are exhibited at Table. 1 [35].

GPD	$\alpha(0)$	$\alpha'[\text{GeV}^{-2}]$	$b[\text{GeV}^{-2}]$	$N^u$	$N^d$
$\bar{E}_T$	-0.1	0.45	0.67	29.23	21.61
$H_T$	-	0.45	0.04	0.68	-0.186

Table 1: Regge parameters and normalizations of the GPDs at a scale of 2 GeV for Model-2.

Results of this model are shown at COMPASS energies in Fig. 2 by dashed lines. It can be seen that there are some discrepancy between Model-2 results and COMPASS data [16] at large  $-t > 0.3\text{GeV}^2$ . That was the reason to test in addition the new Model-3 results for  $\pi^0$  and  $\eta$  leptonproduction. The parameters for new Model-3 are listed at Table. 2 [35]. Note that in this model parameters are close to model I in [25], only parameters of  $\bar{E}_T$  was changed. It can be seen from the  $N$  parameters that Model-2 have larger  $\bar{E}_T$  and smaller  $H_T$  values with respect to Model-3. In Model-3, we have smaller  $\bar{E}_T$  and larger  $H_T$ . Both models describe well  $\pi^0$  production at COMPASS. Model-3 gives better results for large  $-t > 0.3\text{GeV}^2$ , see Fig. 2.

Model-2 and 3 results for  $\pi^0$  production at CLAS energy are exhibited in Fig. 3. It can be seen that both models are in accordance with unseparated cross sections

GPD	$\alpha(0)$	$\beta^u$	$\beta^d$	$\alpha' [\text{GeV}^{-2}]$	$b [\text{GeV}^{-2}]$	$N^u$	$N^d$
$\bar{E}_T$	-0.1	4	5	0.45	0.77	20.91	15.46
$H_T$	-	-	-	0.45	0.3	1.1	-0.3

Table 2: Regge parameters and normalizations of the GPDs at a scale of 2 GeV. Model-3.

$\sigma = \sigma_T + \epsilon\sigma_L$ , where  $\sigma_T$  predominated. At the same time, Model-3 gives closer results for  $\sigma_{TT}$  that is smaller with respect to Model-2. This confirms mentioned before smaller value of  $\bar{E}_T$  in the Model-3.  $\sigma_{LT}$  cross sections are shown as well.

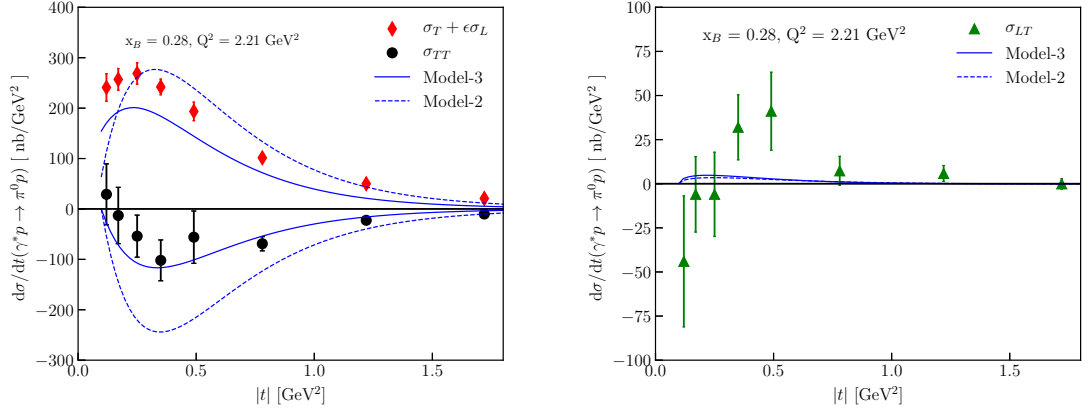


Figure 3: Cross sections of  $\pi^0$  production in the CLAS energy range together with the data [15]. Left graph is for  $\sigma$  and  $\sigma_{TT}$  while right graph is for  $\sigma_{LT}$ .

Calculation of the amplitudes of  $\eta$  production is similar to the  $\pi^0$  case and based on the [27] results where the singlet-octet decomposition of  $\eta$ -state was used with redefined decay constants.

The flavor factors for  $\pi^0$  and  $\eta$  production are appear in combinations

$$\begin{aligned}
F_{\pi^0} &= \frac{1}{\sqrt{2}}(e^u F^u - e^d F^d) = \frac{1}{3\sqrt{2}}(2F^u + F^d); \\
F_{\eta} &= \frac{1}{\sqrt{6}}(e^u F^u + e^d F^d) = \frac{1}{3\sqrt{6}}(2F^u - F^d).
\end{aligned} \tag{9}$$

The  $\eta$  factor is written without strange sea contribution which is small and can be neglected.

From Table 1 and 2, it can be seen that  $\bar{E}_T$  has the same signs for  $u$  and  $d$  quarks but  $H_T$  has the different signs, respectively. This means that for  $\pi^0$  case  $\bar{E}_T$

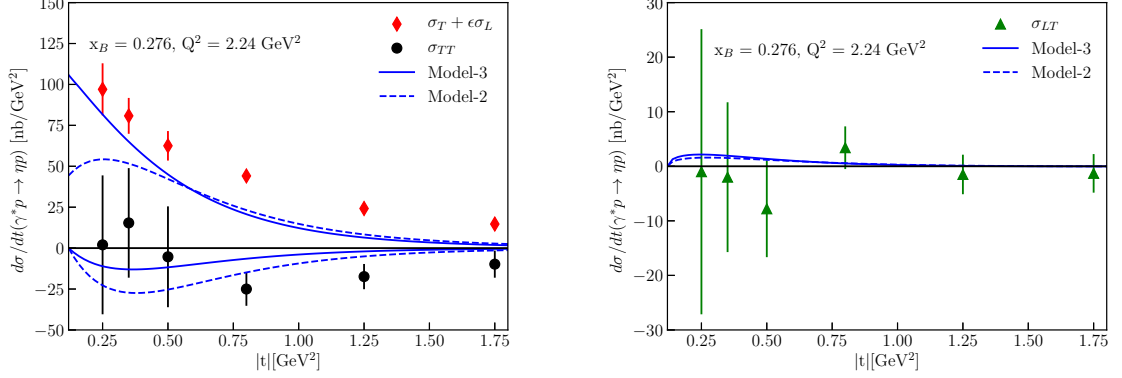


Figure 4: Cross section of  $\eta$  production in the CLAS energy range together with the data [17]. Left graph is for  $\sigma$  and  $\sigma_{TT}$  while right graph is for  $\sigma_{LT}$ .

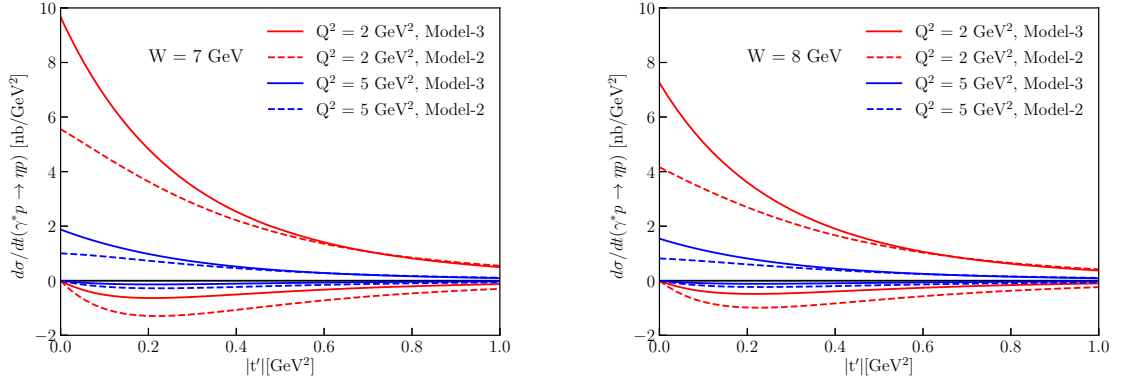


Figure 5: Cross sections of  $\eta$  production at EicC energy. Upper part of the figure presents  $\sigma = \sigma_T + \epsilon \sigma_L$  and down part-  $\sigma_{TT}$  as in Fig. 4.

contributions for  $u, d$  quarks are added but  $H_T$  are subtracted. For  $\eta$  production we have opposite case:  $H_T$  contributions are added but  $\bar{E}_T$  compensated.

Thus we have  $\bar{E}_T$  enhancement for  $\pi^0$  case. For  $\eta$  production  $H_T$  is increasing. Therefore,  $\pi^0$  process is more sensitive to  $\bar{E}_T$  effects but for  $\eta$  production  $H_T$  influences are more visible.

Models results for  $\eta$  production at CLAS energy [17] are depicted in Fig. 4. It can be seen that Model-3 with larger  $H_T$  contribution describes experimental data better at small momentum transfer. Model-2 with smaller  $H_T$  produces essential dip in the cross section that is not observed at experiment. Cross sections  $\sigma_{TT}$  and  $\sigma_{LT}$  are described properly for both models.

Model-2 predictions at EicC energies for  $\pi^0$  production are presented at [25].



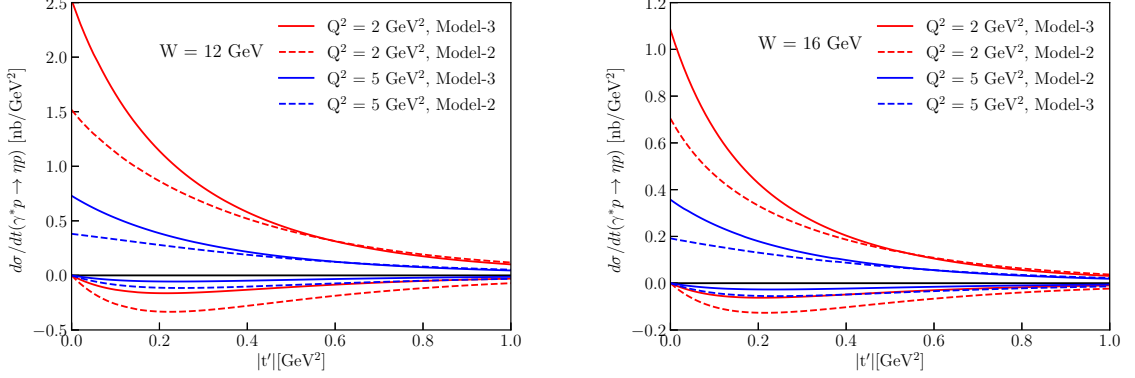


Figure 6: Cross section of  $\eta$  production at EicC energy. The labels are same as in Fig. 5.

For Model-3 at these energies we have results similar to shown in Fig. 2. The  $\pi^0$  cross sections for Model-3 don't have deep near  $|t'| = 0$  GeV<sup>2</sup> as we have for Model-2. Model-2 and 3 results are similar for  $|t'| \sim 0.2$  GeV<sup>2</sup> and cross section is a bit smaller for Model-3 with respect to Model-2 at  $|t'| > 0.3$  GeV<sup>2</sup>.

Our results for EicC energies  $W = 7-16$  GeV for  $\eta$  production are exhibited in the Figs. 5 and 6. It can be concluded that Model-3 results are higher for the cross section  $\sigma$  with respect to Model-2 and for  $\sigma_{TT}$  result is opposite- Model-2 gives higher results. This is caused by larger  $H_T$  contribution in Model-3 and larger  $\bar{E}_T$  effects in Model-2 that is important in  $\sigma_{TT}$ . These model results can be checked experimentally by EicC and determine what Model-2 or 3 is more adequate to experiment.

Now we shall discuss how we can get information about transversity convolutions  $\bar{E}_T$  and  $H_T$  from experimental data. From Eq. (1), we can obtain

$$\begin{aligned}
 |M_{0+++}| &= \sqrt{-\kappa \frac{d\sigma_{TT}}{dt}}, \\
 |M_{0-++}| &= \sqrt{2\kappa \left( \frac{d\sigma_T}{dt} + \frac{d\sigma_{TT}}{dt} \right)},
 \end{aligned} \tag{10}$$

we can determine the absolute values of the amplitudes. Employing normalization factor from Eq. (3) we can determine  $H_T$  and  $\bar{E}_T$  convolutions. This procedure was adopted to extract transversity convolutions from CLAS experimental data in Ref. [28, 29].

Now we don't have experimental data from China EicC. To demonstrate what can be done we shall use instead realistic experimental data, our model calculations for the cross sections  $\frac{d\sigma_T}{dt}$  and  $\frac{d\sigma_{TT}}{dt}$ . Our results for  $H_T$  and  $\bar{E}_T$  convolutions for  $\pi^0$  and  $\eta$  production are depicted in Fig. 7. They are close to results found in [28, 29]

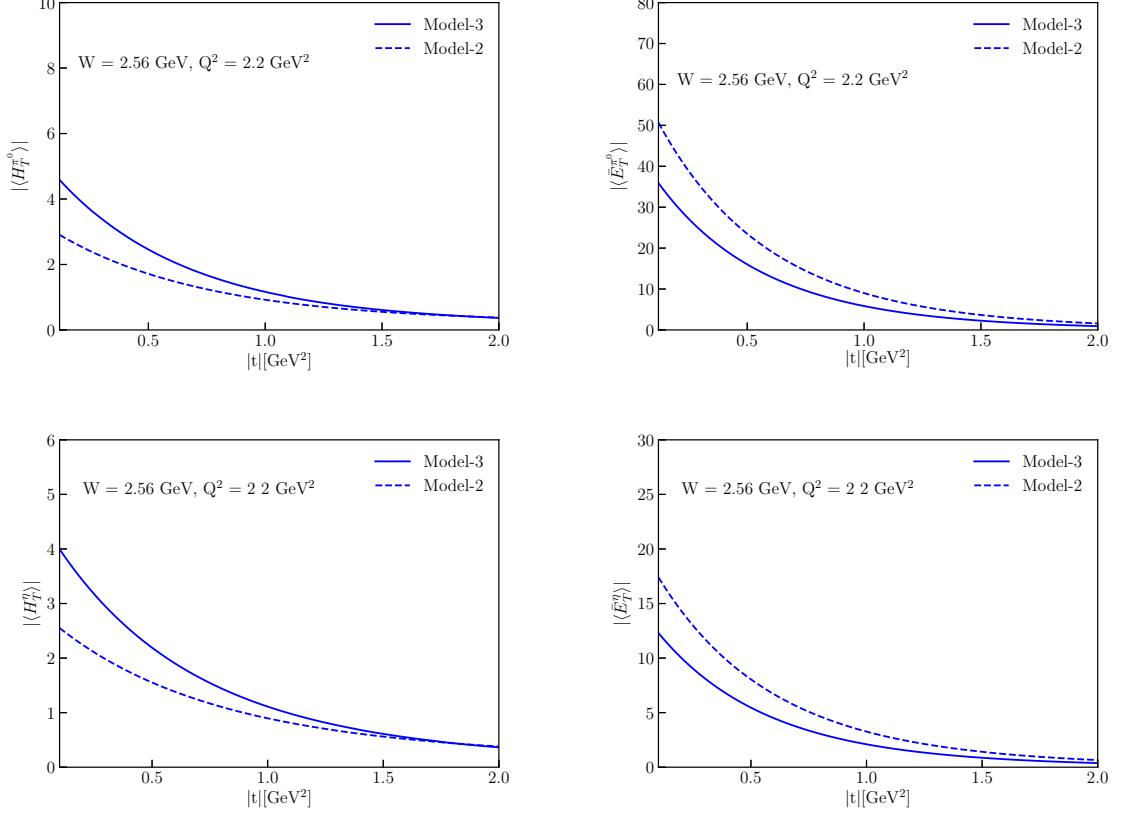


Figure 7: Extracted from the cross section transversity convolutions  $|\langle H_T \rangle|$  and  $|\langle \bar{E}_T \rangle|$  for  $\pi^0$  (upper part) and  $\eta$  production (lower part) at CLAS energy range.

at CLAS energies. As expected we find that  $H_T$  convolution is larger for Model-3, at the same for Model-2 we get larger  $\bar{E}_T$ . Using these results, we can extract convolutions for  $u$  and  $d$  flavors under the help of:

$$\begin{aligned}
 F^u &= \frac{3}{4}(\sqrt{2}F^\pi + \sqrt{6}F^\eta), \\
 F^d &= \frac{3}{2}(\sqrt{2}F^\pi - \sqrt{6}F^\eta),
 \end{aligned} \tag{11}$$

which is a consequence of Eq. (9). Here  $F$  are corresponding transversity  $H_T$  or  $\bar{E}_T$  convolution functions. Such analyzes was performed at CLAS energies at [29].

We will not do this here, because we have model results for flavor convolutions, but extraction of transversity convolution functions from future experimental data can be in important result in later experiments.

Our predictions for  $H_T$  or  $\bar{E}_T$  convolution functions that were extracted from the cross sections at the energies  $W = 8, 12$  GeV which are typical at EicC energy

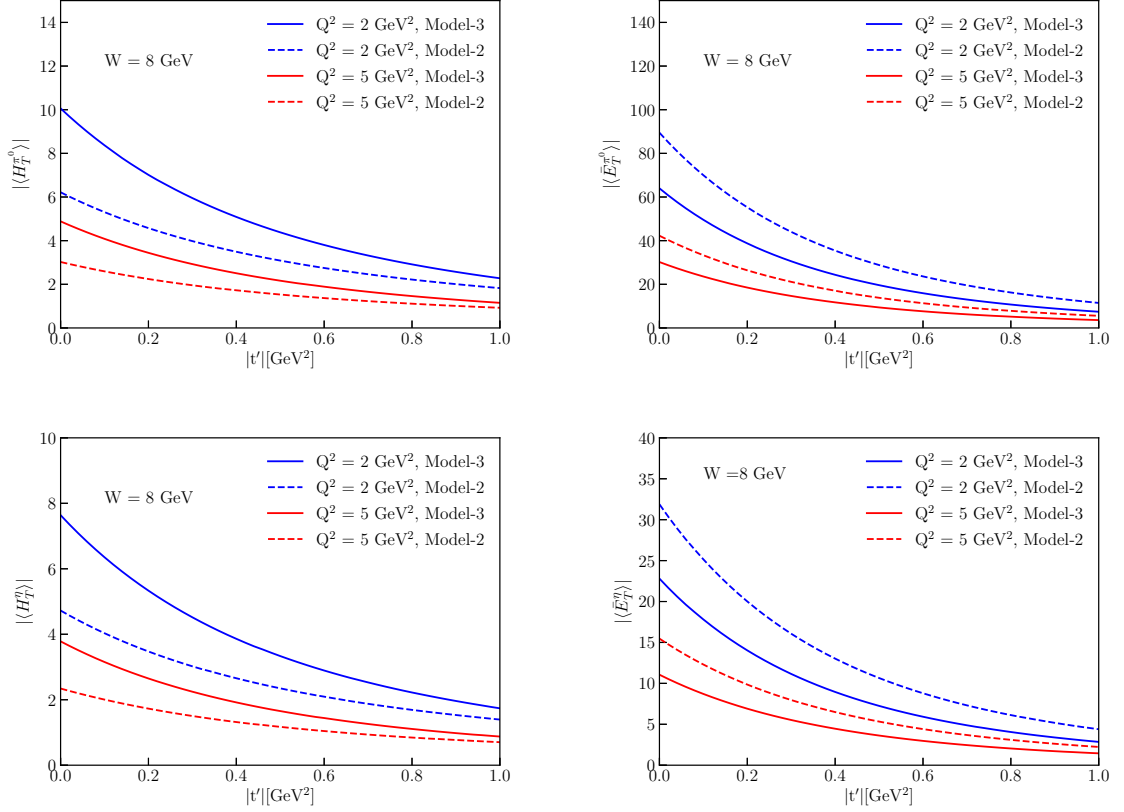


Figure 8: Extracted from the cross section transversity convolutions for  $\pi^0$  (upper part) and  $\eta$  (lower part) production at EicC ( $W = 8$  GeV).

range are exhibited in Figs. 8 and 9. Experimental analyses of these quantities can give information on the preferable models for transversity GPDs.

In Fig. 10, we present our model predictions for energy dependencies of transversity convolution functions at fixed  $Q^2$  and momentum transfer. Such analyses will be important to give a constraints on the  $W$ -dependence of  $H_T$  or  $\bar{E}_T$  GPDs from future experimental data.

Note that the transversity dominance  $\sigma_T \gg \sigma_L$  that was tested for  $\pi^0$  production at high energies is valid for  $\eta$  production at the energies  $W = 2 \sim 15$  GeV. This means that in experimental analyzes of transversity convolutions, unseparated cross section  $\sigma = \sigma_T + \epsilon \sigma_L$  can be applied instead  $\sigma_T$  for both processes of  $\pi^0$  and  $\eta$  production.

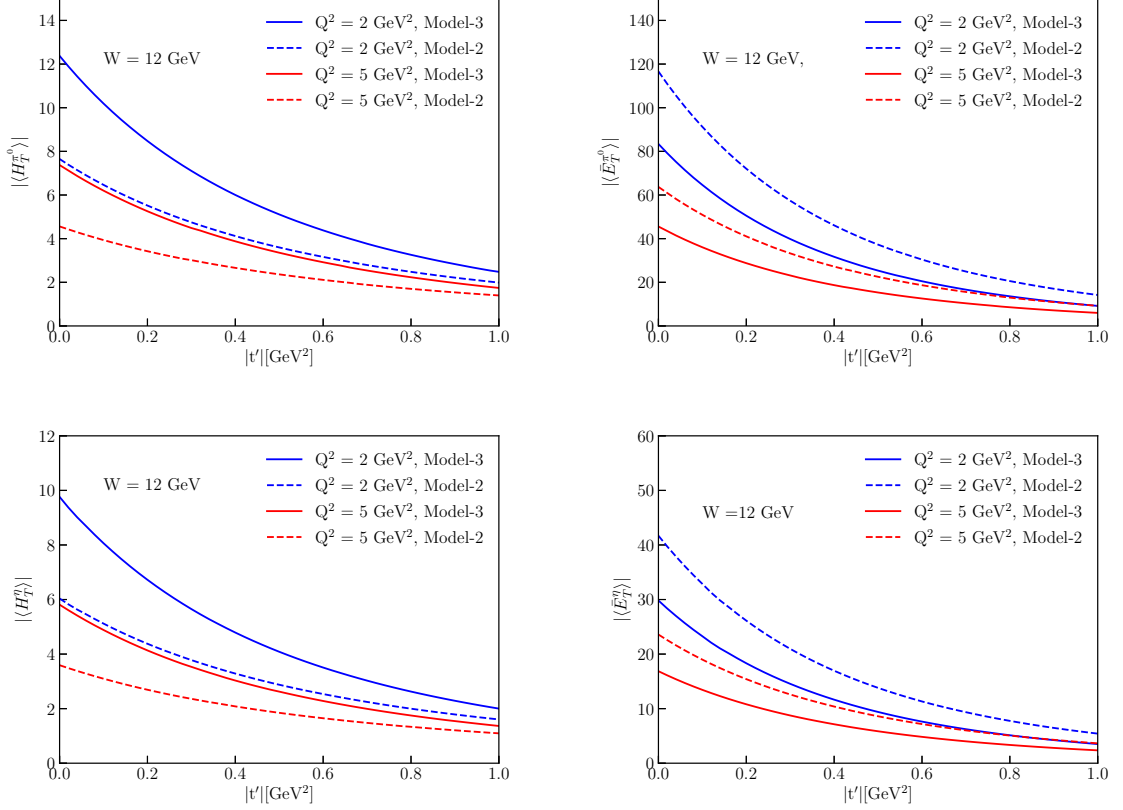


Figure 9: Extracted from the cross section transversity convolution functions for  $\pi^0$  (upper part) and  $\eta$  (lower part) production at EicC ( $W = 12$  GeV).

## 4 Conclusion

In this paper we investigate exclusive electroproduction of pseudoscalar  $\pi^0$  and  $\eta$  meson at China EicC energies. The process amplitudes are calculated in the model where amplitudes are factorized into subprocess amplitudes and GPDs. For the transversity twist-3 effects, the subprocess amplitude  $\mathcal{H}_{0-,++}$  is the same in Eq. (8) for both contributions that contains  $H_T$  and  $\bar{E}_T$  GPDs.

We consider two GPDs parameterization Model-2 and Model-3. Both models describe properly  $\pi^0$  and  $\eta$  production at CLAS energies. It seems that Model-3 gives better results for  $\pi^0$  production at COMPASS at large momentum transfer and gives better description of  $\eta$  production at CLAS at momentum transfer  $|t| < 0.5$  GeV<sup>2</sup>.

We perform predictions for unseparated  $\sigma$  and  $\sigma_{TT}$  cross sections for EicC kinematics for  $\eta$  production with Model-2 and Model-3. We observe that transversity dominance  $\sigma_T \gg \sigma_L$ , found at low CLAS energies [27] and confirmed at EicC

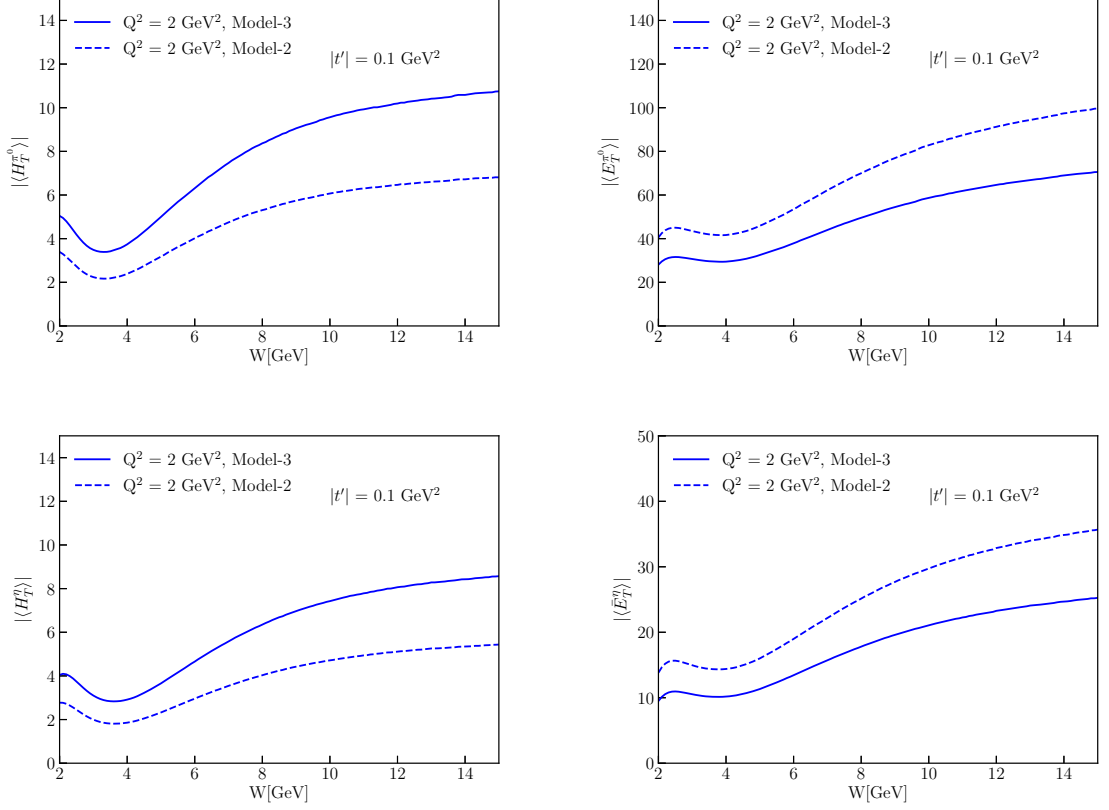


Figure 10: Energy dependencies of extracted transversity convolutions for  $\pi^0$  (upper part) and  $\eta$  (lower part) production at EicC ( $Q^2 = 2 \text{ GeV}^2$ ,  $|t'| = 0.1 \text{ GeV}^2$ ).

energies in Ref.[25] for  $\pi^0$  process is valid at all these energies for  $\eta$  production too.

Adopting combination of the cross sections, we extract GPDs  $H_T$  and  $\bar{E}_T$  convolutions determined in Eq. (3) for the cases of  $\pi^0$  and  $\eta$  mesons. These results for EicC energies are quite different that give possibility to determine preferable model at future experiments. In addition, we analyze energy dependencies of transversity convolutions at fixed  $t$  and  $W$  that can give information about energy parameters of GPDs  $H_T$  and  $\bar{E}_T$  from the data.

Note that reactions  $\pi^0$  and  $\eta$  production considered here have different flavor contributions to the amplitudes. This gives possibility to perform  $u$  and  $d$  flavor separation for transversity GPDs [29].

Our results can be useful in future experiments at China EicC on the pseudoscalar mesons production and give more important knowledge on transversity influences at these energy ranges.

## Acknowledgment

S.G. expresses his gratitude to P.Kroll for collaboration on GPDs study and to V.Kubarovsky for important discussions. The work partially supported by is Strategic Priority Research Program of Chinese Academy of Sciences (Grant NO. XDB34030301) and the CAS president's international fellowship initiative (Grant No. 2021VMA0005).

## References

- [1] D. Müller, D. Robaschik, B. Geyer, F. M. Dittes and J. Hořejši, Fortsch. Phys. **42**, 101-141 (1994) [arXiv:hep-ph/9812448 [hep-ph]].
- [2] X. D. Ji, Phys. Rev. Lett. **78**, 610-613 (1997) [arXiv:hep-ph/9603249 [hep-ph]].
- [3] A. V. Radyushkin, Phys. Lett. B **385**, 333-342 (1996) [arXiv:hep-ph/9605431 [hep-ph]].
- [4] X. D. Ji, Phys. Rev. D **55**, 7114-7125 (1997) [arXiv:hep-ph/9609381 [hep-ph]].
- [5] M. Constantinou, A. Courtoy, M. A. Ebert *et al.* Prog. Part. Nucl. Phys. **121**, 103908 (2021) [arXiv:2006.08636 [hep-ph]].
- [6] K. Goeke, M. V. Polyakov and M. Vanderhaeghen, Prog. Part. Nucl. Phys. **47**, 401-515 (2001) [arXiv:hep-ph/0106012 [hep-ph]].
- [7] M. Vanderhaeghen, P. A. M. Guichon and M. Guidal, Phys. Rev. D **60**, 094017 (1999) [arXiv:hep-ph/9905372 [hep-ph]].
- [8] M. Diehl, Phys. Rept. **388**, 41-277 (2003) [arXiv:hep-ph/0307382 [hep-ph]].
- [9] A. V. Belitsky and A. V. Radyushkin, Phys. Rept. **418**, 1-387 (2005) [arXiv:hep-ph/0504030 [hep-ph]].
- [10] A. V. Radyushkin, Phys. Rev. D **56**, 5524-5557 (1997) [arXiv:hep-ph/9704207 [hep-ph]].
- [11] J. J. C. Collins, L. Frankfurt and M. Strikman, Phys. Rev. D **56**, 2982-3006 (1997) [arXiv:hep-ph/9611433 [hep-ph]].
- [12] E. R. Berger, M. Diehl and B. Pire, Eur. Phys. J. C **23**, 675-689 (2002) [arXiv:hep-ph/0110062 [hep-ph]].
- [13] B. Pire, L. Szymanowski and J. Wagner, Phys. Rev. D **79**, 014010 (2009) [arXiv:0811.0321 [hep-ph]].

- [14] D. Mueller, B. Pire, L. Szymanowski and J. Wagner, Phys. Rev. D **86**, 031502 (2012) [arXiv:1203.4392 [hep-ph]].
- [15] I. Bedlinskiy *et al.* [CLAS], Phys. Rev. C **90**, no.2, 025205 (2014) [arXiv:1405.0988 [nucl-ex]].
- [16] M. G. Alexeev *et al.* [COMPASS], Phys. Lett. B **805**, 135454 (2020) [arXiv:1903.12030 [hep-ex]].
- [17] I. Bedlinskiy *et al.* [CLAS Collab], Phys.Rev.C **95** 035202 (2017) [arXiv:1703.06982 [nucl-ex]].
- [18] A. Accardi, J. L. Albacete, M. Anselmino *et al.* Eur. Phys. J. A **52**, no.9, 268 (2016) [arXiv:1212.1701 [nucl-ex]]. R. Abdul Khalek, A. Accardi, J. Adam *et al.* [arXiv:2103.05419 [physics.ins-det]].
- [19] D. P. Anderle, V. Bertone, X. Cao *et al.* Front. Phys. (Beijing) **16**, no.6, 64701 (2021) [arXiv:2102.09222 [nucl-ex]].
- [20] X. Chen, F. K. Guo, C. D. Roberts and R. Wang, Few Body Syst. **61**, no.4, 43 (2020) [arXiv:2008.00102 [hep-ph]].
- [21] J. M. M. Chávez, V. Bertone, F. De Soto Borrero *et al.* Phys. Rev. Lett. **128**, no.20, 202501 (2022) [arXiv:2110.09462 [hep-ph]].
- [22] I. V. Musatov and A. V. Radyushkin, Phys. Rev. D **61**, 074027 (2000) [arXiv:hep-ph/9905376 [hep-ph]].
- [23] S. V. Goloskokov and P. Kroll, Eur. Phys. J. C **42**, 281-301 (2005) [arXiv:hep-ph/0501242 [hep-ph]]. Eur. Phys. J. C **50**, 829-842 (2007) [arXiv:hep-ph/0611290 [hep-ph]]. Eur. Phys. J. C **59**, 809-819 (2009) [arXiv:0809.4126 [hep-ph]].
- [24] S. V. Goloskokov and P. Kroll, Eur. Phys. J. C **65**, 137-151 (2010) [arXiv:0906.0460 [hep-ph]].
- [25] S.V. Goloskokov, Ya-Ping Xie and Xurong Chen. e-Print: 2206.06547 [hep-ph]
- [26] M. Defurne *et al.* [Jefferson Lab Hall A], Phys. Rev. Lett. **117**, no.26, 262001 (2016) [arXiv:1608.01003 [hep-ex]].
- [27] S. V. Goloskokov and P. Kroll, Eur. Phys. J. A **47**, 112 (2011) [arXiv:1106.4897 [hep-ph]].
- [28] P. Kroll, Few Body Syst. **57**, 1041-1050 (2016), [arXiv:1602.03803 [hep-ph]]
- [29] V. Kubarovsky, Int.J.Mod.Phys.Conf.Ser. **40**, 166005 (2016) [arXiv:1601.04367 [hep-ex]]; PoS SPIN2018 07 (2019) [arXiv:1902.02643 [hep-ph]]

- [30] J. Botts and G. F. Sterman, Nucl. Phys. B **325**, 62-100 (1989)
- [31] R. Jakob and P. Kroll, Phys. Lett. B **315**, 463-470 (1993) [erratum: Phys. Lett. B **319**, 545 (1993)] [arXiv:hep-ph/9306259 [hep-ph]]. J. Bolz, P. Kroll and J. G. Korner, Z. Phys. A **350**, 145-159 (1994) [arXiv:hep-ph/9403319 [hep-ph]].
- [32] J. Pumplin, D. R. Stump, J. Huston *et al.* JHEP **07**, 012 (2002) [arXiv:hep-ph/0201195 [hep-ph]].
- [33] M. Diehl, T. Feldmann, R. Jakob and P. Kroll, Eur. Phys. J. C **39**, 1-39 (2005) [arXiv:hep-ph/0408173 [hep-ph]].
- [34] B. Berthou, D. Binosi, N. Chouika *et al.* Eur. Phys. J. C **78**, no.6, 478 (2018) [arXiv:1512.06174 [hep-ph]].
- [35] P.Kroll, private communication, (2019).



